



Cronfa - Swansea University Open Access Repository

This is an author produced version of a paper published in : *Journal of Applied Ecology*

Cronfa URL for this paper: http://cronfa.swan.ac.uk/Record/cronfa32982

Paper:

Péron, G., Fleming, C., Duriez, O., Fluhr, J., Itty, C., Lambertucci, S., Safi, K., Shepard, E., Calabrese, J. & Bauer, S. (2017). The energy landscape predicts flight height and wind turbine collision hazard in three species of large soaring raptor. *Journal of Applied Ecology* http://dx.doi.org/10.1111/1365-2664.12909

This article is brought to you by Swansea University. Any person downloading material is agreeing to abide by the terms of the repository licence. Authors are personally responsible for adhering to publisher restrictions or conditions. When uploading content they are required to comply with their publisher agreement and the SHERPA RoMEO database to judge whether or not it is copyright safe to add this version of the paper to this repository. http://www.swansea.ac.uk/iss/researchsupport/cronfa-support/

Received Date : 02-Dec-2016

Accepted Date : 21-Mar-2017

Article type : Standard Paper

Editor : Silke Bauer

The energy landscape predicts flight height and wind turbine collision hazard in three species of large soaring raptor

Guillaume Péron (1,2)#

Chris H. Fleming (1,3) Olivier Duriez (4) Julie Fluhr (4) Christian Itty (5) Sergio Lambertucci (6) Kamran Safi (7) Emily L.C. Shepard (8) Justin M. Calabrese (1,3)

- (1) Smithsonian Conservation Biology Institute, National Zoological Park, Front Royal, Virginia 22630, USA
- (2) Univ Lyon, Université Lyon 1, CNRS, Laboratoire de Biométrie et Biologie Evolutive UMR5558, F-69622 Villeurbanne, France
- (3) Department of Biology, University of Maryland, College Park, Maryland 20742, USA
- (4) Centre d'Ecologie Fonctionnelle et Evolutive, UMR 5175 CNRS-Université de Montpellier-EPHE-Université Paul Valery, 1919 Route de Mende, 34293 Montpellier cedex 5, France
- (5) ONCFS SD34, Les Portes du Soleil, 147 route de Lodève, 34 990 Juvignac, France
- (6) Grupo de Biología de la Conservación, Laboratorio Ecotono, INIBIOMA (CONICET– Universidad Nacional del Comahue), Quintral 1250, 8400 Bariloche, Argentina

This article has been accepted for publication and undergone full peer review but has not been through the copyediting, typesetting, pagination and proofreading process, which may lead to differences between this version and the Version of Record. Please cite this article as doi: 10.1111/1365-2664.12909

- (7) Max Planck Institut für Ornithologie, Am Obstberg 1, 78315 Radolfzell, Germany
- (8) Swansea Laboratory for Animal Movement, Biosciences, College of Science, Swansea University, Singleton Park, Swansea SA2 8PP, Wales, United Kingdom

corresponding author: peron_guillaume@yahoo.fr Running title: Modelling flight height of soaring raptors

Summary

- 1. Collisions of large soaring raptors with wind turbines and other infrastructures represent a growing conservation concern. We describe a way to leverage knowledge about raptor soaring behaviour to forecast the probability that raptors fly in the rotor-swept zone. Soaring raptors are theoretically expected to select energy sources (uplift) optimally, making their flight height dependent on uplift conditions. This approach can be used to forecast collision hazard when planning or operating wind farms. Empirical investigations of the factors influencing flight height have however so far been hindered by observation error.
- 2. We propose a two-pronged approach. First, we fitted state-space models to z-axis GPS tracking data to filter heavy-tailed observation error and estimate the relationship between vertical movement parameters and weather variables describing the energy landscape (thermal and orographic uplift potential). Second, we fitted a mechanistic model of flight height above-ground based on aerodynamics and resource selection theories. The approach was replicated for five GPS-tracked Andean condors *Vultur gryphus*, eight griffon vultures *Gyps fulvus*, and six golden eagles *Aquila chrysaetos*.
- 3. In all individuals, movement parameters correlated with thermal uplift potential in the expected direction. In all species, collision hazard was lowest for high thermal uplift potential values. Species-specificities in the presence of a peak in collision hazard for medium values of thermal uplift potential could be explained by differences in wing loading and aspect ratio.
- 4. *Synthesis and applications*. Our fitted models convert weather data (thermal uplift potential) into a prediction of collision hazard (probability to fly in the rotor-swept zone), making it possible to prioritize different wind development projects with respect to the relative hazard they would pose to raptors. However, our model should be combined

with post-construction monitoring to document, and eventually account for turbine avoidance behaviours in collision rate predictions.

Key-words: flight height, movement ecology, 3D, human-wildlife conflict, wind turbines, wind power, continuous-time, raptor, state-space models, z-axis GPS tracking data

Introduction

Large raptors extract energy from the atmosphere to sustain long-distance flight (Pennycuick 1971; Duriez *et al.* 2014). They primarily use two types of uplift: orographic uplift, corresponding to the rise in elevation of air masses above rising terrain, and thermal uplift, corresponding to convection cells caused by small-scale heterogeneity in solar heat absorption and storage by the surface of the Earth. At any given time, the "energy landscape" can thus be characterized by the distance between thermals, the vertical velocity of air masses inside thermals, plus the relief features that create orographic uplift in combination with wind direction and speed (Shepard *et al.* 2013).

How this energy landscape controls collision risk with human infrastructure and aircraft has received little attention so far, yet this information is critical to minimize the effect of infrastructures on wildlife populations, and in particular the effect of wind farms (Barrios & Rodríguez 2004; Vasilakis *et al.* 2016). Because of the conjunction of several vulnerability factors (slow pace of life, relatively poor manoeuvrability when soaring, tendency to focus on the ground below them rather than surveying for threats above and in front), soaring raptors are especially at risk from wind power developments. In fact, the viability of some populations is already jeopardized by this new source of mortality (Carrete *et al.* 2009). Soaring raptors, however, have high public profiles and provide recognized ecosystem services, setting the stage for a rapidly emerging controversy. In that context, an

evidence-based strategy to inform wind farm siting decisions and to manage the operation of existing facilities has been developed, based on a predictive model of collision risk that is periodically updated as new data about actual collisions are collected, analysed, and compared to predictions (Péron *et al.* 2013; New *et al.* 2015; Katzner *et al.* 2016). That framework has been tailored to and focused on golden eagles (*Aquila chrysaetos*) in the USA, so there remains a knowledge gap for most species and regions. To fill that gap, we propose a protocol to analyse the flight height of GPS-tracked raptors in order to predict the probability that they will fly in the rotor-swept zone of wind turbines, a proxy for collision hazard (Katzner *et al.* 2012). We aimed to predict collision hazard as a function of environmental covariates across the landscape, in a way that can readily be reproduced and applied across species and places. To do so, we based our approach on a combination of remotely-sensed and weather data that is available for most locations on Earth (in particular via movebank.org; Wikelski & Kays 2016).

The proposed protocol is two-pronged. First, we dealt with observation error: z-axis GPS data are typically much noisier than xy-axes GPS data, and, combined with error in the digital elevation model used to estimate where the ground is below the flying bird (see "Analysis step 1" in the Methods section), this high rate of error represented an immediate and unavoidable challenge to the estimation of collision hazard. Indeed, in this study, about 36% of our raw flight height records were classified as underground (negative height). Discarding negative flight height records would substantially reduce the sample size, would introduce a problematic skew in the distribution of errors and would artificially select only the records that are far from the ground, thereby massively biasing the inference about flight height. Proper treatment of observation error was therefore required before any inference about vertical space use could be made (Blackwell 1997; Jonsen, Flemming &

Myers 2005; Johnson *et al.* 2008; Pozdnyakov *et al.* 2014). We fitted a continuous-time stochastic movement model (Blackwell 1997; Johnson *et al.* 2008; Fleming *et al.* 2014a) within a state-space framework (de Valpine & Hastings 2002), in order to "filter out" the observation error from our flight height data (Albertsen *et al.* 2015). We also used the state-space analysis to estimate the link between vertical movement parameters and covariates that describe the energy landscape, to validate these covariates as ecologically meaningful in this context. We expected that the mean flight height would increase, the volatility would increase, and the temporal autocorrelation of flight height would decrease with uplift speed (see "Uplift potential metrics" in the Methods section).

In a second step, we used the flight heights, corrected for observation error, as input in a nonlinear regression to estimate the parameters of a mechanistic model of collision hazard. To derive this model, we used the framework laid out for birds by Pennycuick (2008) based on theory developed for glider planes by MacCready (1958), and we combined it with a resource selection function representing the expected switch from orographic to thermal uplift when thermal uplift speed changes (see "Analysis step 2" in the Methods section). We applied the methodology to five Andean condors (*Vultur gryphus*), eight griffon vultures (*Gyps fulvus*), and six golden eagles (Table 1). These three species have markedly different foraging strategies, wing loading, and aspect ratio, so we expected the sensitivity of flight height to thermal uplift condition to decrease from the condor to the eagle. We eventually outlined how our mechanistic model of collision hazard can inform management strategies.

Material and methods

DATA COLLECTION

We collected long-term time series of flight height records from GPS-tracked birds, using a relatively coarse sampling resolution (1-15 minute intervals) but long monitoring durations (4-28 months) to capture change in flight behaviour over time (e.g., with seasonal variation in uplift conditions).

For five juvenile condors, GPS units (Table 1) were duty-cycled to transmit their position in 3D (longitude, latitude, and elevation above the Earth reference ellipsoid) every day from dawn to dusk every 15 minutes. We kept the data collected between 11:00 and 15:00 ART, because preliminary data examination indicated that the birds are almost always airborne during that time. Importantly, we did not filter the data with respect to recorded flight height, only by time of day.

For eight adult vultures, the loggers (Table 1) were programmed to collect their position in three dimensions every day from dawn to dusk every 1 - 5 minutes. The data were downloaded by Bluetooth connection when birds where coming to a feeding station. Based on preliminary examination of the accuracy of altitude measurements, we selected only the records obtained when 6 or more satellites were available. We kept the data collected between 9:00 and 16:00 CET.

For six adult eagles, the loggers (Table 1) were solar-powered and programmed to collect their position in three dimensions every day from dawn to dusk every 1 - 15 minutes (depending on season and solar radiation). The data were downloaded by UHF transmission close to the nest or roost site. Contrary to vultures and condors, eagles spend >50% of time perched during the day. We therefore used horizontal displacement between two records as

an indicator of whether the bird was flying. We discarded records that were less than 15 meters apart from the previous record (a.k.a. immobility threshold). We also discarded data collected before 8:00 and after 17:00 CET. Note that the adult eagles in this study are range-resident throughout the year (no marked seasonal migration).

For all birds and species in this study, between the last record of one day and the first record of the next day, the individual roosted for the night, i.e., each day represented a separate flight path (Fig. 1).

UPLIFT POTENTIAL METRICS

We used uplift potential metrics derived by Bohrer *et al.* (2012) to characterize the energy landscape at any given time. These metrics are, dimensionally speaking, velocities. They scale to the expected speed of thermal convection and of orographic uplift.

Thermal uplift potential, a.k.a. convective velocity scale (Wyngaard 2010), is computed as a function of temperature, pressure, height of the atmospheric boundary layer, and surface sensible heat flux as provided by regional models based on a network of balloon and ground weather station data (Bohrer *et al.* 2012). The spatial resolution of this computation is 32 km and its temporal resolution is 3 hours. Thermal uplift potential scales to the expected speed of convection (Stull 1988). The convection is fastest when the heating from the ground is most vigorous, when the air temperature is coldest, and when the atmospheric boundary layer is highest. However thermal convection cells remain turbulent by nature. They vary at scales finer than the spatial and temporal resolutions of the thermal uplift potential computation. For this reason, there was initially no guarantee that thermal uplift potential would be of any value for applications like those presented in this study (Bohrer *et al.* 2012; Katzner *et al.* 2012). We used the regression between thermal uplift

potential and individual-specific movement parameters as a validation of the ecological meaningfulness of thermal uplift potential (see "Analysis step 1" below).

Orographic uplift potential is computed from a digital elevation model and wind speed and direction interpolations (Bohrer *et al.* 2012). Preliminary analyses indicated that orographic uplift potential did not relate to any of the quantities we investigated in this study (Fig. S2 in Appendix S1; see also "Orographic uplift potential" in the Discussion section). Orographic uplift potential was therefore not further analysed nor directly employed in the modelling framework below.

ANALYSIS STEP 1: CONTINUOUS-TIME STOCHASTIC MOVEMENT MODELS WITH OBSERVATION ERROR

Flight height was measured as the difference between the GPS-derived flight height above ellipsoid, and the ground elevation above sea level extracted from a digital elevation model. This simple operation yielded a metric that accumulated (at least) four sources of error: 1) error on latitude and longitude GPS positioning, flawing the coupling between flight height and ground elevation data, 2) error on the remote-sensed ground elevation data used to generate the digital elevation model, 3) ground elevation interpolation error (Gorokhovich & Voustianiouk 2006; Januchowski *et al.* 2010), and 4) error on the GPS-based measure of flight height above ellipsoid, which itself is slightly different from flight height above sea level. Each type of error encompasses multiple non-independent events, such as interactions between relief features, between relief and weather, between interpolation error and satellite availability, etc. The propagation of these non-independent sources of error is thus expected to create heavy tails in the distribution of the error term, much in the way that the multiplication of Gaussian variables creates a non-Gaussian heavy-tailed variable

(Mitzenmacher 2004). Heavy tails are a source of bias in statistical analyses when they occur but are ignored (Lange, Little & Taylor 1989). Gel, Miao & Gastwirth's (2007) SJ-test applied to the raw data was significant in all birds (P< 0.01), indicating that heavy tails occurred in the distribution of the process variance, the observation variance, or both, which our modelling approach addresses (see below). No skewness was visually detected using QQplots.

We employed a state-space model to systematically separate the variance in flight height data into a process component (the actual vertical movements) and a sampling component (observation error) (Blackwell 1997; de Valpine & Hastings 2002; Jonsen, Flemming & Myers 2005; Johnson et al. 2008), and thereby estimate the flight height in order to assess collision hazard. In this study, the state process was a one-dimensional continuous-time stochastic movement model (a.k.a. correlated random walk). Based on the semivariogram of the flight height time series (Fig. 2: A, E, I), we used the Ornstein-Uhlenbeck position process (OU-p), which is bounded to a finite domain (Blackwell 1997; Fleming *et al.* 2014b). OU-p models are described by parameter μ representing the mean position of the process (the height towards which the birds are reverting to), parameter τ representing the characteristic position autocorrelation time (the rate at which the birds revert to their mean flight height after a random deviation), and parameter σ representing the volatility rate, which is akin to the initial diffusion rate for small time lags (the rate at which deviations from the mean occur). We enforced the loss of temporal autocorrelation in flight height from one day to the next by drawing the first flight height of each day from a normal distribution with the same mean as the OU-p process, and a between-day variance parameter to be estimated jointly with the parameters of the within-day OU-p process. Our state-space approach was developed in the context of medium temporal resolutions (5-30

minute intervals), i.e., when there is potentially more than one change in flight behaviour between two subsequent flight height records (cf. "Method discussion" in the Discussion section).

To investigate how flight behaviour varied with uplift conditions and validate uplift potential metrics as ecologically relevant, the parameters of the OU-p process were made to vary log-linearly with thermal uplift potential. We expected that the process mean flight height (μ) would increase with thermal uplift potential, modelling reversion towards higher heights above ground when thermal uplift is faster. The volatility rate (σ) was expected to increase with thermal uplift potential, and the autocorrelation time (τ) to decrease, modelling faster and more frequent changes in flight height above-ground when thermal uplift was faster. This effect of thermal uplift potential also effectively incorporated a seasonal effect into the movement models, because thermal uplift potential is strongly seasonal in the study regions (preliminary results not shown). Including such covariate effects into the OU-p model also accommodated potential departures from the purely Gaussian distribution, i.e., heavy tails in the distribution of process variance.

The observation process was assumed to follow a generalized Student's t-distribution with a mean equal to the actual position of the bird, a scale parameter to be estimated, and v degrees of freedom ($v \ge 3$, to be estimated). v controlled the heaviness of the tails of the distribution of the observation variance.

We used Template Model Builder (TMB; Kristensen *et al.* 2014) to fit this state-space model to flight height track records separately for each individual bird. We provide in Appendix S2 the C++ and R scripts to fit our model by likelihood maximization and test the approach with simulated data.

Likelihood optimization, even with simple movement models, is increasingly recognized as a challenge not to be underestimated by movement ecologists (Auger-Méthé et al. 2016). This issue stems from both the well-known difficulty to optimize multidimensional problems (Varadhan 2014), and from the specificity of movement models, such as the large statistical covariance between volatility and autocorrelation time (Blackwell 1997; Fleming et al. 2014a). In this study, we found it most efficient to 1) perform the optimization in several steps, i.e., first fit a model without covariate effects (fixing corresponding parameters to zero using the "map" option in TMB objects), and then to estimate each parameter separately (μ , σ , and τ in this order) while fixing the others to their best values so far. 2) We used the BFGS algorithm in R because the Nelder-Mead algorithm almost systematically converged towards saddle points (with non-invertible hessians) or encountered issues of non-estimable gradients, which seems to be an ongoing issue with TMB objects around saddle points. For two problematic datasets, we used 30 generations of a genetic algorithm with derivative (Mebane & Sekhon 2011) in order to weed out saddle points. 3) The choice of the initial input for the position time series was very important to obtain a global maximum. We tried the following initial values: the mean recorded height above-ground, a moving average with window 5 plus random deviation of 5 meters, and a moving average with window 20 plus random deviation of 40 meters. The first option performed best for the vultures and eagles, and the third option best for the condors.

Importantly, flight height above-ground must obviously be positive, but the Laplace approximation framework employed by TMB requires that the focal variable is distributed between + and $-\infty$. To implement the constraint that flight height is strictly positive, we employed a custom link function, denoted *g* (Eq. 1). This technique is like the use of the *log* link in the generalized linear model framework, but contrary to *log*, *g* is almost linear over

most of its domain. See Appendix S1 (section 2) for fuller justification and comparison with other candidate link functions.

Eq. 1
$$z' = g(z; B) = \begin{cases} z & \text{if } z \ge B \\ B + B \cdot \operatorname{atanh}(z/B - 1) & \text{if } z < B \end{cases}$$

where atanh denotes the hyperbolic arctangent, a standard mathematic function with well-characterized properties, and *B* is a fixed parameter (taken as B = 4 meters in our study). The state process acted on the transformed scale (z' variable). The z' variable was back-transformed before applying the observation process. Thereby, all negative flight height records were considered erroneous, and helped inform the amount of error in the observation process.

We investigated whether the two innovations proposed in this section (the generalized Student's t-distribution of observation error and the custom link function) improved the fit compared to what would have been available otherwise (the Gaussian distribution of observation error and the log link function) in a single condor individual using the Akaike Information Criterion (AIC = deviance + twice the number of parameters). Both features were found to greatly improve the model fit for that individual (>100 AIC points differences). Based on this preliminary result, we decided to use these two model features for all individuals without further assessment of model fit.

ANALYSIS STEP 2: COMPUTATION OF COLLISION HAZARD

In step 1 we generated a probabilistic estimate of the modal flight heights at the time of the records, corrected for observation error. We transformed these into a time series of Boolean variables featuring zeros when the birds were flying out of the zone that a turbine rotor would sweep (should a turbine exist), and ones when the birds were flying in the rotor-swept zone. We then fitted a mechanistic model to these data.

To derive this mechanistic model, we used the framework laid out for birds by Pennycuick (2008) based on theory developed for glider planes by MacCready (1958). Initially, we assumed that thermals were not a limiting resource, i.e., a bird could always find a thermal within reach. In this simple model, birds moved cross-country (i.e., laterally) by gliding from thermal to thermal, and used thermal uplift to regain the potential energy they lost during the glides (Akos, Nagy & Vicsek 2008; Appendix S1, section 1). Following previous authors, we denoted *w* the thermal uplift speed, *h* the flight height at which the bird left the current thermal to glide towards the next thermal (or its final destination), v_x the gliding velocity of the bird on the horizontal plane, and v_z the sinking rate of the bird when gliding (negative, vertical velocity component).

During each thermal ascension phase, the bird spent a time $t_1 = a/w$ in the rotorswept zone, where *a* is the span of the turbine blades and *w* is the thermal uplift speed, i.e., the vertical velocity of the bird in the thermal (Fig. S1 in Appendix S1). To also characterize the time spent outside of the rotor-swept zone, we assumed a linear relationship between optimal thermal exit height h^* and thermal uplift speed *w*, following Shepard *et al.* (2011) (we rescaled Shepard et al.'s relationship using the range of observed flight height values in our study species). Throughout, an asterisk indicates the optimal value of a variable, e.g., h^* denotes optimal thermal exit height.

During each gliding phase, the bird spent a time $t_2 = a/v_z$ in the rotor-swept zone (Fig. S1 in Appendix S1). From McCready's (1958) theory there is a generic relationship between the two velocity components, the gliding polar curve p such that: $v_z^* = p(v_x^*)$. By assuming that the bird minimized the time spent in flight when traveling between two

locations (see also Horvitz *et al.* 2014), we got, as explained by e.g., Akos, Nagy & Vicsek (2008):

Eq.2

$$\frac{p(v_x^*) - w}{v_x^*} = p'(v_x^*)$$

where p' is the derivate of the gliding polar curve p. If one has an analytical form for p, Eq. 2 can be solved for v_x^* , yielding a formula for v_x^* as a function of w only. We used the quadratic parameterization of p given by Pennycuick (2008), populated with wing shape and body weight data using Pennycuick's (2008) 'Flight' software. Condor and vulture morphometrics were measured on the same individuals that were GPS-tracked in this study, while eagle morphometrics were taken out of the 'wing database' of the Flight software.

When flying cross country over a distance *D*, the bird in this model spent a time $t = \frac{D}{L} \cdot (t_1 + t_2)$ in the rotor-swept zone, where *L* is the cross-country distance travelled during one iteration of the thermal soaring / inter-thermal gliding process (Fig. S1). There is a simple trigonometric relationship between *L*, *h** and **v*** (Fig. S1). Replacing the formula for t_1 , t_2 , and *L* in the equation for *t*, we got that $t = D \cdot a \cdot \left(\frac{1}{w} + \frac{1}{v_2^*}\right) \cdot \frac{v_2^*}{v_x^* \cdot h^*}$. Further replacing v_2^* by the polar curve, *h** by its linear relationship with *w*, and v_x^* by its relationship with *w* (derived from Eq. 2), we obtained that the time spent in the rotor-swept zone per unit of cross-country distance travelled depends solely on the thermal uplift speed *w* [m/s] and on the span of the turbine blades *a* [m] (Eq. 3).

Eq.3
$$t_{risk}(a, w) = a \cdot \frac{p(v_x^*(w)) + w}{h^*(w) \cdot w \cdot v_x^*(w)}$$

This equation now needed to be modified to account for occasions when thermals were not available or were less profitable than other sources of uplift. To do so, we assumed that the bird planned as if thermals were always available, but when that proved not to be the case,

it switched to orographic uplift. In other words, in our model, orographic uplift acted as a back-up energy source in the absence of thermal uplift.

When flying in orographic uplift, we could assume that 1) the effect of terrain decreased with height above-ground, yielding a low upper bound for flight height above-ground when riding orographic uplift (Shepard, Williamson & Windsor 2016); 2) in orographic currents, the bird simply followed the terrain and therefore maintained a relatively constant flight height above-ground (Katzner *et al.* 2015). Whether this behaviour in orographic currents translates into a decrease or increase in collision hazard compared to when alternating between thermal soaring and gliding is likely to be situation-specific (Johnston *et al.* 2014; Miller *et al.* 2014; our results). We modified Eq. 3 by introducing the proportion θ of time spent riding orographic uplift, modelled, as is commonplace in resource selection theory, with a logistic function: $\theta = \frac{1}{1+e^{\frac{W-W50}{Wr}}}$, where w_r [m/s] represents the rate at which a change in thermal uplift speed translates into a change in the proportion of time spent using orographic uplift, and w_{50} [m/s] denotes the thermal

and half is spent riding orographic uplift. Combining this model of resource selection and Eq. 3, we expressed the probability of flying in the rotor-swept zone as R(a, w) in Eq. 4.

uplift speed for which half the time is spent alternating between thermal soaring and gliding,

Eq.4

$$R(a,w) = \frac{c_0}{1+e^{\frac{w-w_{50}}{w_r}}} + \left(1 - \frac{1}{1+e^{\frac{w-w_{50}}{w_r}}}\right) \cdot (t_{risk}(a,w) \cdot c_1 + c_2)$$

with t_{risk} as in Eq. 3. The values of the tuning parameters c_0 [dimensionless], c_1 [s/m], and c_2 [dimensionless], which were estimated from the data jointly with w_r and w_{50} , partly depended on how much more or less dangerous riding orographic uplift was compared to

alternating between thermal soaring and inter-thermal gliding, depending on thermal uplift speed.

To obtain the maximum likelihood estimates of the parameters of Eq. 4, we performed a least squares nonlinear logistic regression. Importantly, we replaced thermal uplift speed in Eq. 4 by thermal uplift potential (cf. "Uplift potential metrics" above), keeping notation *w* for both. The standard errors of parameter estimates were computed by inverting the hessian of the negative log-likelihood of the least squares nonlinear logistic regression model at its minimum. The amount of variation in collision hazard left unexplained by the nonlinear relationship with thermal uplift potential was quantified using McFadden's r² and Somer's D (Appendix S1, section 3).

Results

CONTINUOUS-TIME STOCHASTIC MOVEMENT MODELS

The models attributed a large part of the observed variance in flight height to observation error (estimated standard error of the t distributions: inter-individual mean 95 ± interindividual SD 56 m in condors, 77 ± 11 m in vultures, 152 ± 54 m in eagles). These large estimated standard errors confirmed the need to adequately treat observation error before making inference about vertical space use. As a side note, the difference in error rate between species agreed with differences in the technical capabilities of the different GPS devices and the precision of the digital elevation models. The estimated flight heights were still quite variable after removing observation variance (Figs. 1 & 2). In particular, there were several instances of fast gain in flight height, suggestive of a fast thermal, several instances of gain in height above-ground but loss in absolute elevation above sea level, suggestive of long gliding bouts, and there were periods when the flight height was closely coupled with

the ground elevation, suggestive of soaring in orographic uplift (Fig. 1). As predicted, the process mean μ and the volatility rate σ increased with thermal uplift potential (Table 2), indicating that the average and variance of flight height increased with thermal uplift potential in all species and individuals (Fig. 2: C, G, K). Also as predicted, the autocorrelation time τ decreased with thermal uplift potential in vultures and eagles (negative w effects in Table 2). By contrast, for condors, autocorrelation times were much longer than other species, and did not consistently decrease with thermal uplift potential (inconsistent sign of w effects in Table 2).

COMPUTATION OF COLLISION HAZARD

For Andean condors, collision hazard reached a maximum for intermediate thermal uplift potential values (Fig. 2B), indicating that in this species riding orographic uplift was initially less dangerous than riding thermal uplift, but the reverse was true for high thermal uplift potential values. The switch from orographic to thermal uplift occurred over a relatively small range of thermal uplift speed values ($w_r = 0.20 \pm \text{SD } 0.03 \text{ m.s}^{-1}$) around $w_{50} = 1.5 \pm \text{SD}$ 0.04 m.s⁻¹. For large values of thermal uplift potential, collision hazard decreased because condors increasingly flew above the rotor-swept zone. Large amounts of variation in collision hazard were, however, left unexplained by thermal uplift potential (McFadden's pseudo correlation coefficient: r = 0.15; Somers' index of association: D = 0.20).

For griffon vultures, collision hazard decreased steadily as thermal uplift potential increased (Fig. 2F), indicating that in this species riding orographic uplift was always more dangerous than using thermal uplift. The modelled behavioural switch occurred over a broader range of thermal uplift speed values than in condors ($w_r = 0.41 \pm \text{SD } 0.07 \text{ m.s}^{-1}$) around $w_{50} = 1.25 \pm \text{SD } 0.06 \text{ m.s}^{-1}$. Large amounts of variation in collision hazard were left

unexplained by thermal uplift potential (McFadden's pseudo correlation coefficient: r = 0.16; Somers' index of association: D = 0.21).

For golden eagles, collision hazard showed little variation with thermal uplift potential (Fig. 2J). There was a moderate increase initially, indicating that riding orographic uplift was less dangerous than riding thermals for low thermal uplift potential values. Contrary to the previous two species, the decrease in collision hazard for high values of thermal uplift potential was small (Fig. 2J). This indicated that the flight height of this species was only moderately affected by the availability of thermals. The modelled behavioural switch occurred over the smallest range of thermal uplift speed values of the three species $(w_r = 0.11 \pm \text{SD } 0.02 \text{ m.s}^{-1})$, also quite early at $w_{50} = 0.79 \pm \text{SD } 0.03 \text{ m.s}^{-1}$, but the behaviour switch did not affect flight height very much. Most of the variation in collision hazard was left unexplained by thermal uplift potential (McFadden's pseudo correlation coefficient: r = 0.04; Somers' index of association: D = 0.05).

Discussion

In this study, 36% of raw flight height records were initially classified as underground. This high rate of error, which we believe to be typical of flight height data computed as the difference between the GPS-derived height above ellipsoid and the ground elevation from a digital elevation model, makes it necessary to correct for observation error before inference about vertical space use. We developed a new method, based on the TMB framework (Kristensen *et al.* 2014), to correct flight height above-ground for large, heavy-tailed observation error. In a second step, we used the flight heights, corrected for observation error, to fit a mechanistic model of the probability that large soaring raptors fly in the height zone above ground that would be swept by turbine blades.

VALIDATION OF THERMAL UPLIFT POTENTIAL FOR APPLICATIONS IN CONSERVATION BIOLOGY

Collision hazard was lowest for highest thermal uplift potential values, and that phenomenon was most obvious in the two species most reliant on thermals (condors and vultures). Vertical flight speed (Fig. 2), process mean height (μ ; Table 2), and volatility (σ ; Table 2) consistently and statistically significantly increased with thermal uplift potential in all individuals, as expected if thermal uplift potential is a good proxy for thermal uplift speed. Autocorrelation time decreased with thermal uplift potential also as predicted, although not systematically in condors (τ ; Table 2). The latter result may suggest that flight height is subjected to a different process in condors than in lighter species, especially because a simple resampling exercise indicated that this result is unlikely to come from the coarser sampling schedule of the condors relative to the other species (Fig. S3 from Appendix S1). Overall, our results validated the good performance of thermal uplift potential as a proxy for the actual uplift conditions experienced by the birds. This variable can effectively be used for applications in conservation biology.

OROGRAPHIC UPLIFT POTENTIAL

We offer the following three hypotheses to explain the lack of relationship between the vertical movement rates of soaring birds and orographic uplift potential (Fig. S2 in Appendix S1). First, the wind velocity interpolations upon which the orographic uplift potential computations rest are probably too rough to appropriately represent the conditions that the birds are experiencing. More precise wind velocity data (e.g., embarked airspeed sensors) might in the future make it possible to better address the relationship between wind speed, orographic uplift, and flight behaviour (Taylor, Reynolds & Thomas 2016). Wind speed may also affect flight height through the efficiency of thermal soaring rather than through the

speed of orographic uplift. The most straightforward way to incorporate wind speed into our framework would probably be to make w_r and w_{50} of Eq. 4 vary with wind speed. Ground elevation, another factor entering in the computation of orographic uplift potential, might also influence flight height and collision hazard directly rather than via orographic uplift. For example, our data suggested that eagles flew on average lower above ground when ground elevation was higher (Figs. S4 & S5 in Appendix S1).

Second, when using orographic uplift, soaring birds gain horizontal velocity, but their flight elevation does not vary much (Katzner *et al.* 2015; Shepard, Williamson & Windsor 2016). Since our approach focuses on the vertical component of movement, it is therefore not completely surprising that we did not find any effect of orographic uplift potential.

Third, our model assumes that orographic uplift acted as a "back-up" energy source when thermal uplift was not available or was too slow, i.e., the value of orographic uplift speed is less important than the mere availability of orographic uplift. In other words, the lack of relationship between orographic uplift potential and collision hazard is largely implied by our working hypothesis. To our knowledge, we are the first to formally propose this hypothesis that large soaring birds prioritize between sources of uplift, which was well supported by the condor and vulture data. Lending some additional support to this hypothesis, during migration, soaring birds are known to accumulate along the barriers that delimit areas without orographic uplift, as they await favourable thermal conditions (Miller *et al.* 2016), i.e., soaring birds travelling through environments without orographic uplift are considered to decide not to fly at all when thermal availability is poor (K.S., unpublished data). Note that none of the above three hypotheses negate the importance of orographic

uplift in the ecology of our study species. Indeed, in many parts of their range, these species are restricted to areas where orographic uplift is available.

COMPARISON BETWEEN SPECIES

The collision hazard of eagles did not decrease as much as in the other two species when thermal uplift potential increased. We relate this difference to the lighter weight and lower aspect ratio of eagles compared to vultures and condors, making eagles more willing to use flapping flight and less reliant on thermals than vultures and condors, i.e., more likely to leave thermals before reaching the energetically-optimal height. In addition, being active predators who need to be able to locate and capture small prey, eagles typically maintain a low flight elevation above ground when they are foraging (Watson 2010; Fig. S4 in Appendix S2). By contrast, condors and vultures can reach relatively high elevation above ground while still effectively detecting large carcasses, and they can also use conspecifics to form a network of observers (Deygout *et al.* 2010; Cortés-Avizanda *et al.* 2014).

The comparison between Andean condors and griffon vultures further highlights the role of body mass and wing loading. The heavier weight and greater wing loading of the condor renders the conversion of thermal uplift into potential energy less effective for this species than for vultures (Pennycuick 2008). In support of this, we observed that condors flew on average lower above ground than vultures, that their vertical speed started to increase at much higher thermal uplift potential values than vultures (Fig. 2D vs. 2H), and that they abandoned orographic uplift at higher thermal uplift potential values but more abruptly than vultures (w_{50} and w_r estimates). Overall, condors therefore appeared more reliant on orographic uplift than vultures, and less able to exploit slow thermals, yielding the observed initial increase in collision hazard with thermal uplift potential. When they use

thermals of moderate speed, condors need more iterations of the thermal soaring/interthermal gliding sequence than vultures, and therefore spend more time in the danger zone, explaining the peak in collision hazard at intermediate values of thermal uplift potential.

METHOD DISCUSSION

In this study, we directly analysed the difference between the ground elevation and the flight height above ellipsoid. It could be argued that this approach mixes a time-varying error term (error on flight height) and a time-constant one (error on ground elevation). However, the error on horizontal positioning, although small (a few meters), undoes the association between the digital elevation model and the track records, thereby introducing a time effect on the error on the ground elevation below the bird.

Another particularity of our approach is that the mechanistic model (step 2) was fitted to the output of the stochastic model (step 1), rather than fitting the mechanistic model directly to the data without the stochastic model step. The energy landscape covariate (thermal uplift potential) entered the analytical protocol in the two steps, potentially causing some statistical covariance issues. However, the estimated flight heights were qualitatively similar when step 1 did not include the dependency on thermal uplift potential (preliminary results not shown), so this issue is not believed to affect our results. We are not aware of any study attempting to fit a mechanistic model when the data are both strongly autocorrelated and affected by observation error, although opportunities exist should the data support them (e.g., multistate approaches).

IMPLICATIONS FOR MANAGING THE COLLISIONS OF SOARING BIRDS IN WIND FARMS Our fitted models convert weather data (thermal uplift potential) into a prediction of collision hazard (probability to fly in the rotor-swept zone), making it possible to compare

the relative hazard that different wind development projects would pose to raptors. To further convert collision hazard into collision risk, i.e., the probability that an individual in the study population will collide with a turbine over a given amount of time, two other quantities need to be assessed: 1) the rate at which raptors in the focal population fly over wind farms (a.k.a. raptor use of the wind farms; New et al. 2015), and 2) their avoidance behaviour (i.e., the way in which they modify their flight height in direct response to the presence of wind turbines; Johnston, Bradley & Otter 2014). Under the understanding that risk is the product of hazard and vulnerability, one could term the above two quantities "vulnerability factors". The combination of pre-construction assessments of collision hazard, pre-construction assessments of raptor use of a development area, and post-construction assessment of realized collision rates, could effectively bring information about avoidance behaviour, i.e., the rate at which different species and populations manage to modify their flight behaviour (vertically or horizontally or both) to avoid collision.

In conclusion, GPS tracking data, combined with an understanding of the mechanisms underlying vertical movement, can make it possible to leverage behavioural knowledge for conservation purposes in a situation-tailored way. For wildlife biologists tasked with advising developers and controlling the risk that infrastructures and aircraft pose to large soaring raptors, our results can be used to prioritize potential development areas with respect to the relative hazard they pose.

Authors' contributions

GP conceived the study, conducted the statistical analyses and wrote the first draft. JC obtained funding and co-conceived the study. CF coded the 3D home range estimation. SL, CI, and OD contributed datasets. All authors contributed to the writing of subsequent drafts.

Acknowledgements

The condor study was funded by Agencia Nacional de Promoción Científica y Tecnológica (ANPCYT–FONCYT, PICT(BID) 0725- 2014, Argentina). The vulture study was funded by ANR grant ANR-07-BLAN-0201 (2008-2011), coordinated by F. Sarrazin and C. Bessa-Gomes. This work was supported by the US NSF Advances in Biological Informatics program (ABI-1458748 to JMC). GP was supported by a Smithsonian Institution CGPS grant, and CHF was supported by a Smithsonian Institution postdoctoral fellowship. We warmly thank all the people who participated in data collection and curation.

Data accessibility

Data are not publicly available because they contain sensitive information on endangered species. Data have been uploaded to Movebank, under the ID numbers 26916044 (Andean condors), 156746015 (Griffon vultures), and 166410847 (Golden eagles) and can be requested via Movebank.

Supporting information

Appendix S1: Full derivation of the theoretical collision risk model; Link function considerations; Explanation of the predictive power metrics; Additional figures.

Appendix S2: R and C++ scripts to fit the Ornstein-Uhlenbeck continuous-time stochastic movement model with heavy-tailed observation error and covariate dependencies using Template Model Builder.

References

- Akos, Z., Nagy, M. & Vicsek, T. (2008) Comparing bird and human soaring strategies.
 Proceedings of the National Academy of Sciences of the United States of America, 105, 4139–4143.
- Albertsen, C.M., Whoriskey, K., Yurkowski, D., Nielsen, A. & Flemming, J.M. (2015) Fast fitting of non-Gaussian state-space models to animal movement data via Template Model Builder. *Ecology*, **96**, 2598–2604.
- Auger-Méthé, M., Field, C., Albertsen, C.M., Derocher, A.E., Lewis, M.A., Jonsen, I.D.,
 Flemming, J.M. & Mills Flemming, J. (2016) State-space models' dirty little secrets: even simple linear Gaussian models can have estimation problems. *Scientific reports*, 6, 26677.
- Barrios, L. & Rodríguez, A. (2004) Behavioural and environmental correlates of soaring-bird mortality at on-shore wind turbines. *Journal of Applied Ecology*, **41**, 72–81.
- Blackwell, P.G. (1997) Random diffusion models for animal movement. *Ecological Modelling*, **100**, 87–102.
- Bohrer, G., Brandes, D., Mandel, J.T., Bildstein, K.L., Miller, T.A., Lanzone, M., Katzner, T.,
 Maisonneuve, C. & Tremblay, J.A. (2012) Estimating updraft velocity components over
 large spatial scales: contrasting migration strategies of golden eagles and turkey
 vultures. *Ecology Letters*, **15**, 96–103.
- Calabrese, J.M., Fleming, C.H. & Gurarie, E. (2016) ctmm: An r package for analyzing animal relocation data as a continuous-time stochastic process. *Methods in Ecology and Evolution*, **7**, 1124–1132.

- Carrete, M., Sánchez-Zapata, J.A., Benítez, J.R., Lobón, M. & Donázar, J.A. (2009) Large scale risk-assessment of wind-farms on population viability of a globally endangered longlived raptor. *Biological Conservation*, **142**, 2954–2961.
- Cortés-Avizanda, A., Jovani, R., Doná Zar, J. & Grimm, V. (2014) Bird sky networks: How do avian scavengers use social information to find carrion? *Ecology*, **95**, 1799–1808.
- Deygout, C., Gault, A., Duriez, O., Sarrazin, F. & Bessa-Gomes, C. (2010) Impact of food predictability on social facilitation by foraging scavengers. *Behavioral Ecology*, **21**, 1131–1139.
- Duriez, O., Kato, A., Tromp, C., Dell'Omo, G., Vyssotski, A.L., Sarrazin, F. & Ropert-Coudert, Y. (2014) How cheap is soaring flight in raptors? A preliminary investigation in freely-flying vultures. *PloS one*, **9**, e84887.
- Fleming, C.H., Calabrese, J.M., Mueller, T., Olson, K.A., Leimgruber, P. & Fagan, W.F. (2014a) Non-Markovian maximum likelihood estimation of autocorrelated movement processes. *Methods in Ecology and Evolution*, **5**, 462–472.
- Fleming, C.H., Calabrese, J.M., Mueller, T., Olson, K.A., Leimgruber, P. & Fagan, W.F. (2014b)
 From fine-scale foraging to home ranges: a semivariance approach to identifying
 movement modes across spatiotemporal scales. *The American Naturalist*, **183**, E154-67.
- Fleming, C.H., Fagan, W.F., Mueller, T., Olson, K.A., Leimgruber, P. & Calabrese, J.M. (2015) Rigorous home-range estimation with movement data: A new autocorrelated kerneldensity estimator. *Ecology*, **96**, 1182–1188.
- Gel, Y.R., Miao, W. & Gastwirth, J.L. (2007) Robust directed tests of normality against heavytailed alternatives. *Computational Statistics and Data Analysis*, **51**, 2734–2746.

Gorokhovich, Y. & Voustianiouk, A. (2006) Accuracy assessment of the processed SRTMbased elevation data by CGIAR using field data from USA and Thailand and its relation to the terrain characteristics. *Remote Sensing of Environment*, **104**, 409–415.

- Horvitz, N., Sapir, N., Liechti, F., Avissar, R., Mahrer, I. & Nathan, R. (2014) The gliding speed of migrating birds: slow and safe or fast and risky? (ed M Holyoak). *Ecology Letters*, **17**, 670–679.
- Januchowski, S.R., Pressey, R.L., VanDerWal, J. & Edwards, A. (2010) Characterizing errors in digital elevation models and estimating the financial costs of accuracy. *International Journal of Geographical Information Science*, **24**, 1327–1347.
- Johnson, D.S., London, J.M., Lea, M.-A. & Durban, J.W. (2008) Continuous-time correlated random walk model for animal telemetry data. *Ecology*, **89**, 1208–1215.
- Johnston, N.N., Bradley, J.E. & Otter, K.A. (2014) Increased Flight Altitudes Among Migrating Golden Eagles Suggest Turbine Avoidance at a Rocky Mountain Wind Installation. *PLoS ONE*, **9**, e93030.
- Jonsen, I.D., Flemming, J.M. & Myers, R.A. (2005) Robust state-space modeling of animal movement data. *Ecology*, **86**, 2874–2880.
- Katzner, T., Benett, V., Miller, T., Duerr, A., Braham, M. & Hale, A. (2016) Wind energy
 development : methods for assessing risks to birds and bats pre-construction. *Human–Wildlife Interactions*, **10**, 42–52.
- Katzner, T.E., Brandes, D., Miller, T., Lanzone, M., Maisonneuve, C., Tremblay, J.A., Mulvihill,
 R. & Merovich, G.T. (2012) Topography drives migratory flight altitude of golden eagles:
 Implications for on-shore wind energy development. *Journal of Applied Ecology*, 49,

1178–1186.

- Katzner, T.E., Turk, P.J., Duerr, A.E., Miller, T.A., Lanzone, M.J., Cooper, J.L., Brandes, D.,
 Tremblay, J.A. & Lemaître, J. (2015) Use of multiple modes of flight subsidy by a soaring terrestrial bird, the golden eagle Aquila chrysaetos , when on migration. *Journal of The Royal Society Interface*, **12**, 20150530.
 - Kristensen, K., Nielsen, A., Berg, C.W., Skaug, H. & Bell, B. (2014) TMB: Automatic Differentiation and Laplace Approximation. *Journal of Statistical Software*, **2014**, 1–21.
- Lambertucci, S. a., Alarcón, P. a E., Hiraldo, F., Sanchez-Zapata, J. a., Blanco, G. & Donázar, J.
 a. (2014) Apex scavenger movements call for transboundary conservation policies. *Biological Conservation*, **170**, 145–150.
- Lange, K., Little, R. & Taylor, J. (1989) Robust statistical modeling using the t distribution. Journal of the American Statistical Association, **84**, 881–896.

MacCready, P.B.J. (1958) Optimum Airspeed Selector. Soaring, 10–11.

- Mebane, W.R.J. & Sekhon, J.S. (2011) Genetic Optimization Using Derivatives: The rgenoud package for R. *Journal of Statistical Software*, **42**, 1–26.
- Miller, T.A., Brooks, R.P., Lanzone, M., Brandes, D., Cooper, J., O'Malley, K., Maisonneuve, C.,
 Tremblay, J., Duerr, A. & Katzner, T. (2014) Assessing risk to birds from industrial wind
 energy development via paired resource selection models. *Conservation Biology*, 28, 745–55.
- Miller, R.A., Onrubia, A., Martín, B., Kaltenecker, G.S., Carlisle, J.D., Bechard, M.J. & Ferrer,
 M. (2016) Local and regional weather patterns influencing post-breeding migration
 counts of soaring birds at the Strait of Gibraltar, Spain (ed J Kelly). *Ibis*, **158**, 106–115.

Mitzenmacher, M. (2004) A Brief History of Generative Models for Power Law and Lognormal Distributions. *Internet Mathematics*, **1**, 226–251.

- Monsarrat, S., Benhamou, S., Sarrazin, F., Bessa-Gomes, C., Bouten, W. & Duriez, O. (2013) How Predictability of Feeding Patches Affects Home Range and Foraging Habitat Selection in Avian Social Scavengers? *PLoS ONE*, **8**, e53077.
- New, L., Bjerre, E., Millsap, B., Otto, M.C. & Runge, M.C. (2015) A Collision Risk Model to Predict Avian Fatalities at Wind Facilities: An Example Using Golden Eagles, Aquila chrysaetos. *PloS one*, **10**, e0130978.
- Pennycuick, C.J. (1971) Soaring Behaviour and Performance of Some Birds, Observed from a Motor-Glider. *Ibis*, **114**, 178–218.

Pennycuick, C.J. (2008) *Modelling the Flying Bird*. Elsevier, New York.

- Péron, G., Hines, J.E., Nichols, J.D., Kendall, W.L., Peters, K.A. & Mizrahi, D.S. (2013)
 Estimation of bird and bat mortality at wind-power farms with superpopulation models. *Journal of Applied Ecology*, **50**, 902–911.
- Pozdnyakov, V., Meyer, T., Wang, Y.-B.B., Yan, J. & Inouye, B.D. (2014) On modeling animal movements using Brownian motion with measurement error. *Ecology*, **95**, 247–253.
- Shepard, E.L.C. & Lambertucci, S.A. (2013) From daily movements to population
 distributions: weather affects competitive ability in a guild of soaring birds. *Interface*, **10**, 30130612.
- Shepard, E.L.C., Lambertucci, S. a, Vallmitjana, D. & Wilson, R.P. (2011) Energy beyond food:
 foraging theory informs time spent in thermals by a large soaring bird. *PloS one*, 6,
 e27375.

Shepard, E.L.C., Williamson, C. & Windsor, S.P. (2016) Fine-scale flight strategies of gulls in urban airflows indicate risk and reward in city living. *Philosophical transactions of the Royal Society of London B, Biological sciences*, **371**, 76–93.

- Shepard, E.L.C., Wilson, R.P., Rees, W.G., Grundy, E., Lambertucci, S.A. & Vosper, S.B. (2013)
 Energy landscapes shape animal movement ecology. *The American Naturalist*, **182**, 298–312.
- Stull, R.B. (1988) *An Introduction to Boundary Layer Meteorology*. Kluwer Academic, Dordrecht, NL.
- Taylor, G.K., Reynolds, K. V. & Thomas, A.L.R. (2016) Soaring energetics and glide performance in a moving atmosphere. *Philosophical Transactions of the Royal Society of London B: Biological Sciences*, **371**.
- de Valpine, P. & Hastings, A. (2002) Fitting population models incorporating process noise and obervation error. *Ecological Monographs*, **72**, 57–76.
- Varadhan, R. (2014) Numerical Optimization in R : Beyond optim. *Journal of Statistical Software*, **60**, 1–3.

Vasilakis, D.P., Whitfield, D.P., Schindler, S., Poirazidis, K.S. & Kati, V. (2016) Reconciling endangered species conservation with wind farm development: Cinereous vultures (Aegypius monachus) in south-eastern Europe. *Biological Conservation*, **196**, 10–17.

Watson, J. (2010) The Golden Eagle. A & C Black, London.

Wikelski, M. & Kays, R. (2016) Movebank: archive, analysis and sharing of animal movement data. http://www.movebank.org, accessed on 12/14/2015

Wyngaard, J.C. (2010) Turbulence in the Atmosphere. University Press, Cambridge, UK.

Tables

Table 1: Study species characteristics, trapping and tagging information. Measurements

represent typical variation across age and sex classes.

Species	Study area	Trapp ing perio d	Devices	Individ ual days	Bod Y weig ht (kg)	Wing loadi ng (kg/ m ²)	Asp ect ratio *1	Social foragi ng ^{*2}	Main food source	Referen ces for field method s
Andean condor (<i>Vultur</i> gryphus)	Patago nia, Argenti na (36°44' S, 69°73' W)	2014- 2015	Solar GPS– GSM loggers (Vektortek LLC) attached with backpack (120 g)	1,692	9-14	9-13	7-8	Yes	Carrio n	Shepard & Lambert ucci 2013; Lambert ucci <i>et</i> <i>al.</i> 2014
Griffon vulture (<i>Gyps</i> <i>fulvus</i>)	Grands Causse s, France (44°10' N, 3°08'E)	2010	Battery- powered GPS- Bluetooth loggers Gipsy-2 (Technos mart), attached with leg- loop harness (100 g)	2,697	7-11	7-10	6.5- 7.5	Yes	Carrio n	Monsarr at <i>et al.</i> 2013
Golden eagle (Aquila chrysae tos)	S. Massif Central , France (43°45' N, 3°16'E)	2013- 2014	Solar GPS- GSM-UHF loggers Skua (Ecotone) attached with backpack (50 g)	3,103	4-5	5.5- 8.5	6-7	No	Mediu m- sized mam mals and birds	Hitherto unpublis hed

^{*1}Aspect ratio is the ratio of the wing span to the mean chord (average width of the extended wing; e.g., Pennycuick 2008)

^{*2} (Deygout *et al.* 2010; Cortés-Avizanda *et al.* 2014)

Table 2: Parameter estimates of the Ornstein-Uhlenbeck vertical position process (OU-p). Intercepts ("Intcp.") and slopes of the effect of thermal uplift potential ("w") are given. Autocorrelation times and volatility rates are log-transformed. Individual identification numbers ("indiv#") are for future reference only. Also given are the number of GPS fixes used ("N") and the median time interval between fixes of the same day ("D", in minutes).

	Andear	n condor	s												
	indiv#	autoco log-sca		on time '	τ (min,	volatili log-sca	process mean μ (m)				. N	D			
		Intcp.	SE	w	SE	Intcp.	SE	W	SE	Intc p.	SE	w	SE		
	JVEC K1	5.68	0.32	-0.08	0.20	2.01	0.19	0.69	0.16	123	8	95	31	193 1	1 5
	JVEC K2	10.79	0.99	0.68	0.55	-3.82	0.57	2.35	0.31	-2	1	76	14	288 6	1 5
	JVEC K3	8.59	4.24	-1.53	2.67	2.08	0.12	0.43	0.14	99	6	21 4	55	186 7	1 5
	JVEC K4	7.62	1.98	2.06	1.27	2.17	0.17	0.26	0.17	135	11	34 4	72	127 1	1 5
	JVEC K5	9.66	3.01	3.30	1.87	0.53	0.54	0.17	0.42	50	4	32	28	192 9	1 5
	Griffon vultures														
_	indiv#	autoco log-sca		on time '	τ (min,	volatili log-sca		σ (m.m	nin ^{-1/2} ,	process mean µ (m)			N	D	
	marvi	Intcp.	SE	w	SE	Intcp.	SE	W	SE	Intc p.	SE	w	SE	. IN	U
	TY092 6-2	3.51	0.11	-0.25	0.12	3.74	0.05	0.47	0.04	149	10	80	13	380 6	2

TY142 6	4.46	0.12	-0.28	0.14	3.05	0.04	0.55	0.04	122	8	54	0. 1	446 0	5
TY161 9	2.84	0.17	-0.55	0.17	4.19	0.05	0.37	0.05	172	17	92	23	148 2	1
TY171 9	3.76	0.12	-0.30	0.23	3.61	0.02	0.50	0.01	74	9	35	11	432 7	2
TY217 7	2.71	0.09	-0.04	0.08	4.09	0.03	0.09	0.03	136	8	31	11	327 8	1
TY373 0	3.37	0.08	-0.01	0.06	4.01	0.02	0.27	0.01	169	11	86	15	392 2	2
TY374 5	3.34	0.03	-0.26	0.04	4.13	0.01	0.32	0.01	195	5	69	5	256 88	3
TY448 5	3.16	0.15	-0.17	0.19	4.17	0.05	0.10	0.04	144	22	17	27	126 7	1
Golden	Golden eagles													

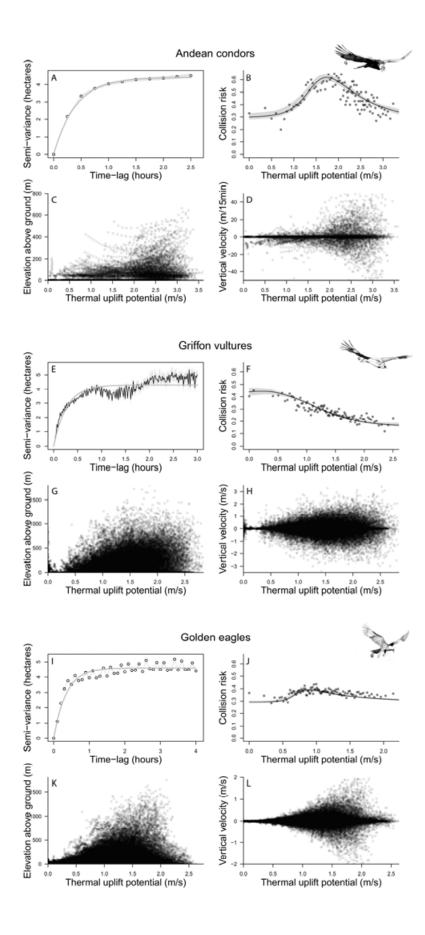
indiv#	autoco log-sca		on time	τ (min,	volatil log-sca	process mean μ (m)				- N	D			
	Intcp.	SE	W	SE	Intcp.	SE	W	SE	Intc p.	SE	w	SE		U
2	4.44	0.10	-0.22	0.11	2.23	0.05	0.41	0.07	7	2	19	3	807 6	1 0
6	4.37	0.16	-0.19	0.17	2.01	0.09	0.50	0.08	-4	3	17	4	292 2	1 5
11	4.06	0.06	-0.04	0.09	3.21	0.03	0.45	0.02	6	4	36	4	114 29	6
12	4.27	0.05	-0.35	0.05	2.53	0.03	0.46	0.03	38	2	22	2	229 85	1 0
14	3.90	0.03	-0.32	0.03	2.98	0.01	0.56	0.03	11	2	22	2	258 94	6
18	3.77	0.04	-0.46	0.04	3.69	0.02	0.64	0.02	128	4	87	5	220 56	6

Figures

Fig. 1: Visualization of the flight data for one adult griffon vulture tracked over 12.2 months. Upper panel: 80% and 95% contours of the 3D kernel density estimate (computed after Fleming et al. 2015; Calabrese, Fleming & Gurarie 2016 and plotted against a digital elevation model by Institut Géographique National). 80% and 95% of the locations fall within the green and blue volumes respectively. The z-axis is magnified 10 times in this panel. The red spheres represent a 48-hour exploration of the outskirts of the home range. The arrow indicates the north and is approximately 5 km long. Lower panel: simplified visualization of the exploration flight represented by red sphere in the upper panel. Red symbols: recorded data (c. one location per minute). Black line: Estimated flight height after removing observation error. This time window was chosen because flight mode switches are easily discernible, but the observation error was lower than average during this time window. Dark grey areas: ground elevation. During the first 40 minutes, the bird is flying near the colony, gaining elevation in thermals or orographic current until it reaches a flight elevation that allows gliding towards the west for the next 40 minutes over 15 km. At the 48th minute of the sequence, the bird picks a thermal and reaches the highest flight height of the sequence within 8 minutes. During the next day (after the vertical bar representing a time ellipse with no data), the flight height is more closely coupled to the ground elevation, suggesting that the bird mostly uses orographic uplift and glides along leeward slopes to get back to the colony.

Fig. 2: (A, E, I): Semivariograms of the z-axis flight height data, averaged over individuals for each species, showing the horizontal asymptote characteristic of rangeresidency. Black line: empirical semivariogram. Grey line: fitted curve showing the

theoretical semivariogram function of an Ornstein-Uhlenbeck position process. Grey area: 95% confidence interval of the semivariogram. Complete details about semivariance theory for movement models are in Fleming et al. (2014). Departures from the theoretical semivariogram are due to variation between individuals (in both their semivariance and the time lags of their time series) and to the stochastic nature of the process. (C, G, K): Relationship between estimated flight height, corrected for observation error using the state-space model, and thermal uplift potential. The mean and variance of flight height both increase with thermal uplift potential. The histogram represents the frequency of thermal uplift potential values along the birds' trajectories. (D, H, L): Relationship between estimated vertical velocity and thermal uplift potential, showing the increase in variance with thermal uplift potential. Vertical velocity is computed as the vertical displacement between to flight height records, corrected for observation error using the state-space model, and divided by the time interval between the records. Note the different scales for each species. (B, F, G): Collision risk. Round symbols: probability of presence in the rotorswept zone (60-180 meters above ground), corrected for observation error and binned into 100 bins of equal size. Solid line: nonlinear logistic regression model predictions based on Eq. 3. Shaded area: 95% confidence interval from a parametric bootstrap with 1000 replicates.



This article is protected by copyright. All rights reserved.

